



## Lectures - Tuesday afternoon, June 10

SL9

### X-RAY DIFFRACTION ANALYSIS OF REFRACTORY MATERIALS USED IN U.S. STEEL KOŠICE

M. Černík, L. Hrabčáková, S. Štulrajter, P. Vranec

U.S. Steel Košice, s.r.o., Vstupný areál U.S. Steel, 044 54 Košice

mcernik@sk.uss.com, lhrabcakova@sk.uss.com, sstulrajter@sk.uss.com, pvranec@sk.uss.com

Different types of refractory materials are used in the refractory lining of the heat aggregates for the steel production. Among the basic raw materials used for their production Corundum ( $\text{Al}_2\text{O}_3$ ), Spinel ( $\text{MgO}\cdot\text{Al}_2\text{O}_3$ ), Periclase ( $\text{MgO}$ ) and others are of great matter. The refractory materials are in direct contact with the slag and steel, where at the interface area, mainly in the case of the slag, the refractory material is directly influenced. This influence is significantly dependent on the type of the refractory material, operational temperature, exposition time and corrosion activity of slag and steel. Generally, by the long-term operation the refractory material is worn, what is not the subject of investigation, but also the structural changes take place. It can be stated that the Corundum is stable and it does not change its crystal structure even after a long-term exposition. Spinel-like structures are however more interesting as the crystal structures is often influenced by additional atoms, where the significant changes in lattice parameters occur. Large amount of measured materials from plant including Spinel structures were divided into

two groups, i.e. castables and castables influenced by slag on its surface.

Standard lattice parameter of the Spinel  $\text{MgAl}_2\text{O}_4$  with the space group  $Fd\bar{3}m$  (227) is according to ICDD card No. 82-2424  $a_0 = 0.80887$  nm and according to ICDD card No. 77-0435  $a_0 = 0.80806$  nm. Materials investigated here include real structures that are often different from the pure materials that are considered as standards. Therefore, the lattice parameter of the Spinel is in many cases different for the analyzed refractory materials containing Spinel from the plant. In many cases of these real materials the presence of two types of Spinel with different lattice parameters was identified. The Spinel structure is in these cases influenced mainly by temperature and chemical elements present in such material. It is necessary to mention that the literature describes the pressure dependence on the lattice parameter. However, our materials are not exposed to high pressures; these are operated at high temperatures and are in contact with liquid iron and liquid slag.

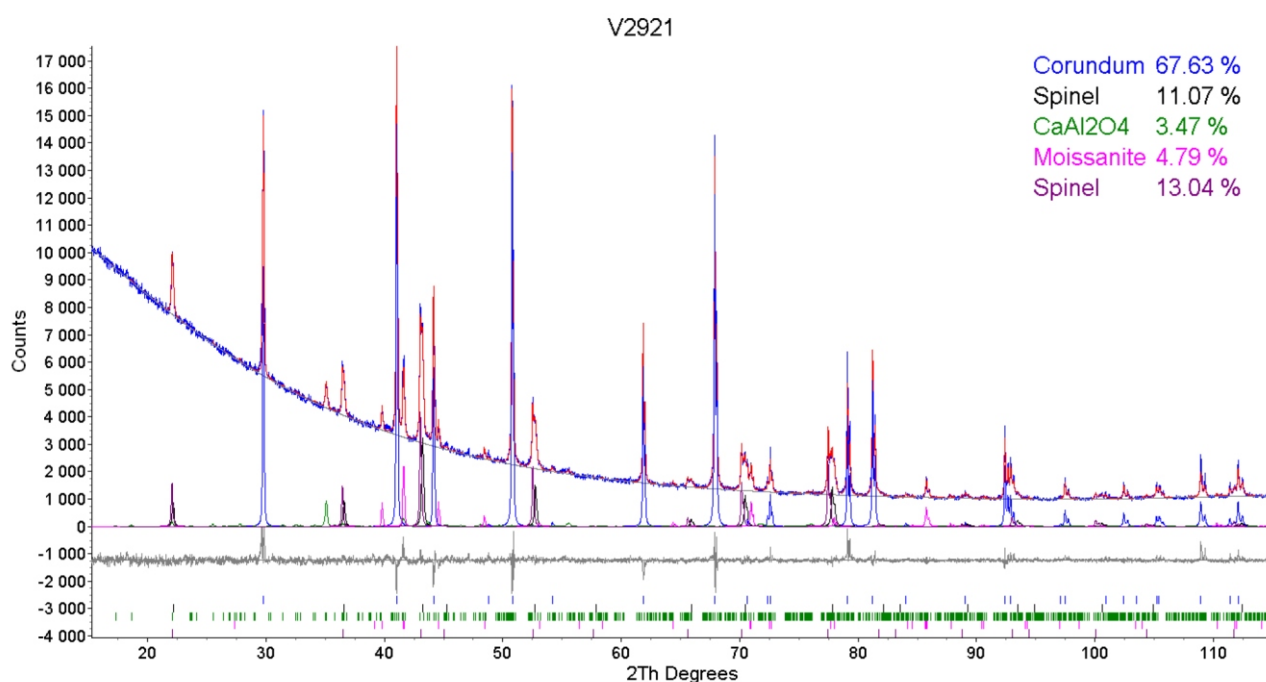
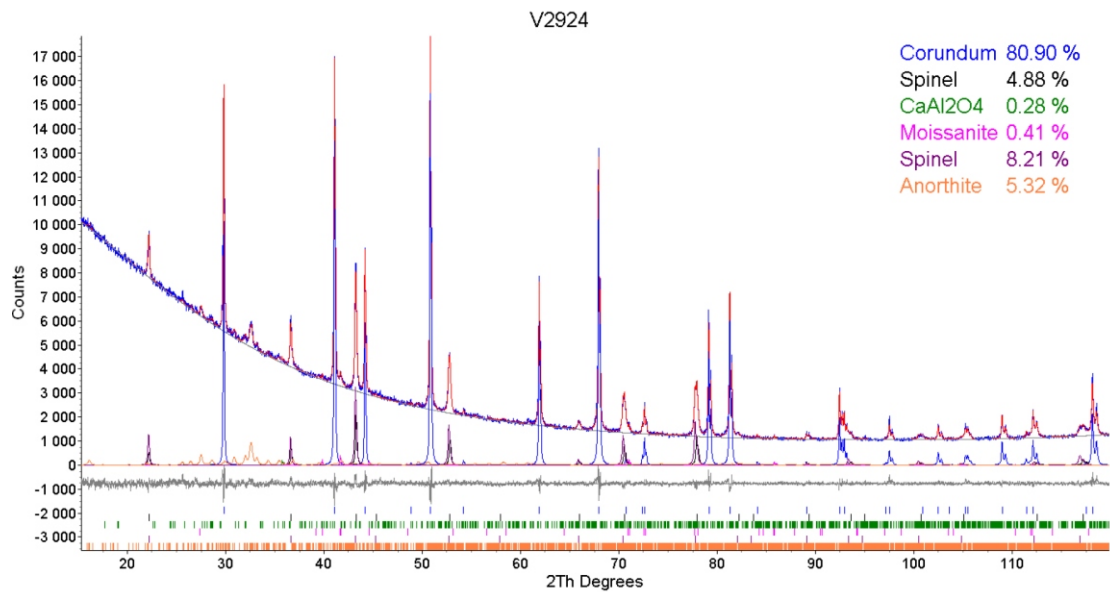


Figure 1. Sample1, detail of the refined diffraction pattern.


**Figure 2.** Sample 2, detail of the refined diffraction pattern.

**Table 1.** Phase compositions of the samples.

| IDENTIFIED PHASE<br>COMPOSITION | Sample 1                | Sample 2    | Sample 3           |             |               |
|---------------------------------|-------------------------|-------------|--------------------|-------------|---------------|
|                                 |                         |             | Mineralogical name | Space Group | Content [wt%] |
| $\text{Al}_2\text{O}_3$         | Corundum                | (167) R-3c  | 67.6               | 80.9        | 77.4          |
| $\text{MgAl}_2\text{O}_4$       | Spinel                  | (227) Fd-3m | 11.1               | 4.9         | 11.1          |
| $\text{MgAl}_2\text{O}_4$       | Spinel                  | (227) Fd-3m | 13.1               | 8.2         | 9.8           |
| $\text{CaAl}_2\text{O}_4$       | Calcium Aluminium Oxide | (014) P21/n | 3.5                | 0.3         | 0.2           |

**Table 2.** The lattice parameters of Spinel and Corundums.

| CHEMICAL FORMULA   | $\text{MgAl}_2\text{O}_4$ | $\text{MgAl}_2\text{O}_4$ | $\text{Al}_2\text{O}_3$ |                   |
|--------------------|---------------------------|---------------------------|-------------------------|-------------------|
| MINERALOGICAL NAME | Spinel                    | Spinel                    | Corundum                |                   |
| SPACE GROUP        | (227) Fd-3m               | (227) Fd-3m               | (167) R-3c              |                   |
| LATTICE PARAMETER  | a [ $10^{-10}$ m]         | a [ $10^{-10}$ m]         | a [ $10^{-10}$ m]       | a [ $10^{-10}$ m] |
| SAMPLE 1           | 8.0546                    | 8.0856                    | 4.7592                  | 12.9923           |
| SAMPLE 2           | 8.0504                    | 8.0643                    | 4.7591                  | 12.9920           |
| SAMPLE 3           | 8.0023                    | 8.0174                    | 4.7589                  | 12.9913           |
| STANDARD           | <b>8.0898</b>             |                           | 4.75                    | 12.982            |

It has been found from many different measured and evaluated data that the lattice parameter in the structure of material which is in contact with liquid slag increases to higher values. The most probable reason is the influence of the slag elements such as Na, Ca, Mg, Al, Si and Fe on the Spinel structure. The lattice parameter takes on higher values which decrease to the standard values by the distance change from surface towards the basic material.

The subject of our investigation was sample including Spinel structure with the lattice parameter of significantly lower value than the standard. Such crystal structure is less described in the literature. The TOPAS software was used for the determination of phase composition content, Fig. 1. Sample 1 contained Corundum, Spinel, Calcium Aluminium Oxide and Silicon Carbide – Moissanite. Tables 1 and 2 show phase composition content and calculated lattice parameter of the Spinel. Table 3 shows the comparison of chemical analysis of Sample 1 with the chemical composition calculated from the phase content.

**Table 3.** The element content recalculated from phase content of samples.

| Sample Analysis | Al [%] | O [%] | Mg [%] | Ca [%] | C [%] | Si [%] | Fe [%] | Ti [%] |
|-----------------|--------|-------|--------|--------|-------|--------|--------|--------|
| 1 - Chem        | 45.9   | 43.9  | 3.4    | 1.1    | 1.3   | 3.3    | 0.03   | 0.05   |
| 1 - X-ray       | 46.2   | 44.2  | 4.2    | 0.9    | 1.5   | 3.4    | -      |        |

For the simulation of the operational characteristics of the material, sample 1 was annealed at 1500 °C 5 hour in the oxidation atmosphere. After the annealing the surface of the sample was black (Sample 2) and few millimeters under the surface the sample remained white (Sample 3). The content of Corundum increased and the content of Spinel, Calcium Aluminium Oxide and Silicon Carbide – Moissanite decreased (Table 1). The formation of Anorthite was observed for the Sample 2. The original sample contained two types of Spinel with different lattice parameters, Table 1. First Spinel with the lattice parameter of  $8.0856 \cdot 10^{-10}$  m can be considered as standard Spinel while the second Spinel with the lattice parameter of  $8.0546 \cdot 10^{-10}$  m cannot be considered as standard. Chemical composition of standard Spinel with the cubic structure can be stated by chemical formula  $MgAl_2O_4$ ; non-standard Spinel, non-stoichiometric  $MgO \cdot nAl_2O_3$ , where  $n = 1.0 - 7.3$  [1]. In the stoichiometric crystals ( $n = 1.0$ ) the  $Mg^{2+}$  ions are in tetrahedral positions and  $Al^{3+}$  ions are mainly in octahedral positions. When the crystal structure deviates from the stoichiometric ratio ( $n > 1$ ) the excess of vacant cations is formed mainly in octahedral positions. By the increase of  $Al_2O_3$  content in the non-stoichiometric Spinel the lattice parameter decreases. The substitution of the tetrahedral  $Mg^{2+}$  ions by  $Al^{3+}$  ions can be described by the following reaction:

SL10

$Mg^{2+} = I_{1/3} + Al^{3+}$ , where  $I_{1/3}$  are the unoccupied vacant cations.

In the limiting case the defect Spinel correspond to  $-Al_2O_3$ . Dependence of the lattice parameter of non-stoichiometric Spinel  $a = f(n)$  was deduced by several authors, see [1].

Annealing in the oxidation atmosphere leads to the reversible transformation of the Spinel to Corundum in the extreme case. Incomplete inversion process leads to non-stoichiometric Spinel  $MgO \cdot nAl_2O_3$ , where the lattice parameter of the Spinel is directly dependent on  $n$ ,  $a = f(n)$ .

Nevertheless, there are still several questions that are unanswered, such as:

- How the physico-metallurgical characteristics of the Spinel depleted by Mg change?
- What are the physico-metallurgical characteristics of the cubic  $-Al_2O_3$  in contrast to Corundum for the extreme case?
- What are the physico-metallurgical characteristics of the Spinel enhanced by elements such as Fe and others?

1. G.I. Belykh, V.T.Gritsyna, L.A.Lytkov, V.B.Kolner: Transformation of spinel crystals structure  $MgO \cdot nAl_2O_3$  under high-temperature annealing, Functional Materials 216, No.3 (2009).

## X-ray and neutron diffraction Study of texture of Zr-samples deformed by uniaxial tension

### STUDIUM TEXTURY ZIRKONIOVÝCH VZORKU DEFORMOVANÝCH JEDNOOSÝM TAHEM POMOCÍ NEUTRONOVÉ A RENTGENOVÉ DIFRAKCE

M. Kučeráková<sup>1</sup>, S. Vratislav<sup>1</sup>, Z. Trojanová<sup>2</sup>

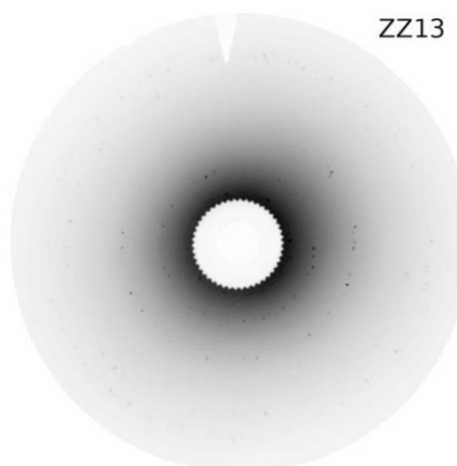
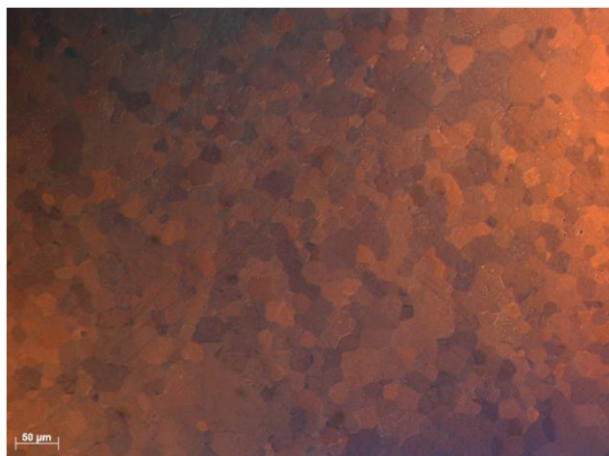
<sup>1</sup>Department of Solid State Engineering, FNSPE CTU in Prague, Trojanova 13, 120 00, Prague, Czech Republic

<sup>2</sup>Department of Physics of Materials, Faculty of Mathematics and Physics, Ke Karlovu 5, 121 16, Prague, Czech Republic  
monika.kruzelova@fffi.cvut.cz

#### Úvod

Pomocí rentgenové a neutronové difrakce byly zkoumány dvě série vzorku čistého  $-Zr$ . První série vzorků byla deformována na trhačce INSTRON 5882 při pokojové teplotě, zatímco druhá série byla deformována při teplotě

300 °C. Obě série byly deformovány od deformace 0 % do deformace 30 %, přičemž deformační krok byl zvolen 5 %. Parametry preferované orientace byly určeny užitím přímých a inverzních pólových obrazců. Neutronografická měření probíhala na difraktometru KSN-2 v Laboratoři



Obrázek 1. Struktura výchozího vzorku - metalografie (vlevo), difrakční obraz - zpětný odraz (vpravo).

neutronové difrakce FJFI ČVUT (umístěné v Řeži u Prahy). Rentgenografická měření probíhala v na theta/theta difraktometru X'Pert PRO. Naměřená data byla zpracována užitím programových balíků GSAS a X'Pert Texture.

### Vzorky

Vzorky z čistého -Zr měly tvar pásku s rozšířenými konci o rozměrech aktivní části 3.3 7 50 mm. Struktura výchozího nedeformovaného vzorku je na obrázku 1 - velikost zrn je cca 20 m.

### Výsledky

Vypočtené hodnoty pólových hustot užitím Harrisova vztahu ve třech významných směrech vzorku zobrazuje obrázek 2. Naměřené přímé pólové obrazce jsou v tabulce 1.

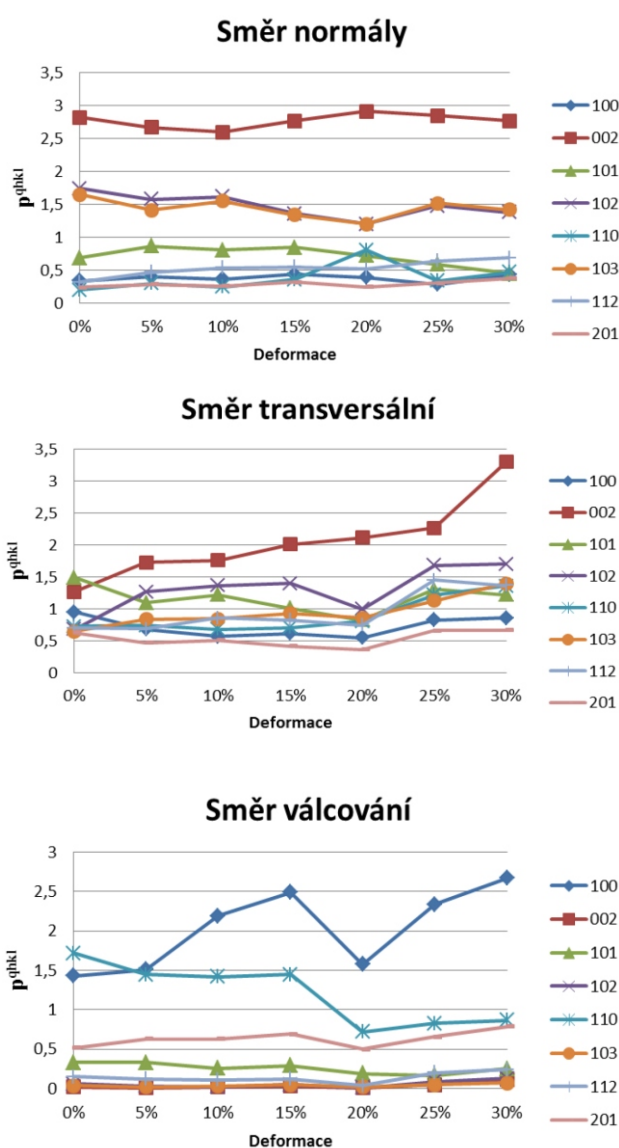
### Diskuze výsledků

Z tabulky 1 lze pozorovat orientaci rovin (002) do směru normály (ND) s tendencí rozšiřovat se o 30° směrem k transversálnímu směru (TD). Srovnatelný výsledek lze získat také z hodnot pólových hustot získaných neutronovou difrakcí pro směr ND (obrázek 2), přičemž je patrné výrazné zvýšení pólové hustoty pro deformaci  $e = 20\%$  ( $p_{002}^{ND} = 2.91$ ).

Kolmo ke směru normály se orientují také roviny (102) a (103), avšak dochází k postupnému slábnutí pólové hustoty. Naopak je pozorovatelný mírný nárůst hustoty pro tyto roviny ve směru transversálním (obrázek 2). Během deformace tedy dochází ke stáčení rovin (102) a (103) od ND směrem k TD.

Z přímých i inverzních pólových obrazců je patrné, že dochází k orientaci rovin (100) kolmo ke směru válcování (obrázek 2). Podobné chování lze pozorovat také pro roviny (110), avšak pólová hustota postupně klesá (obrázek 2).

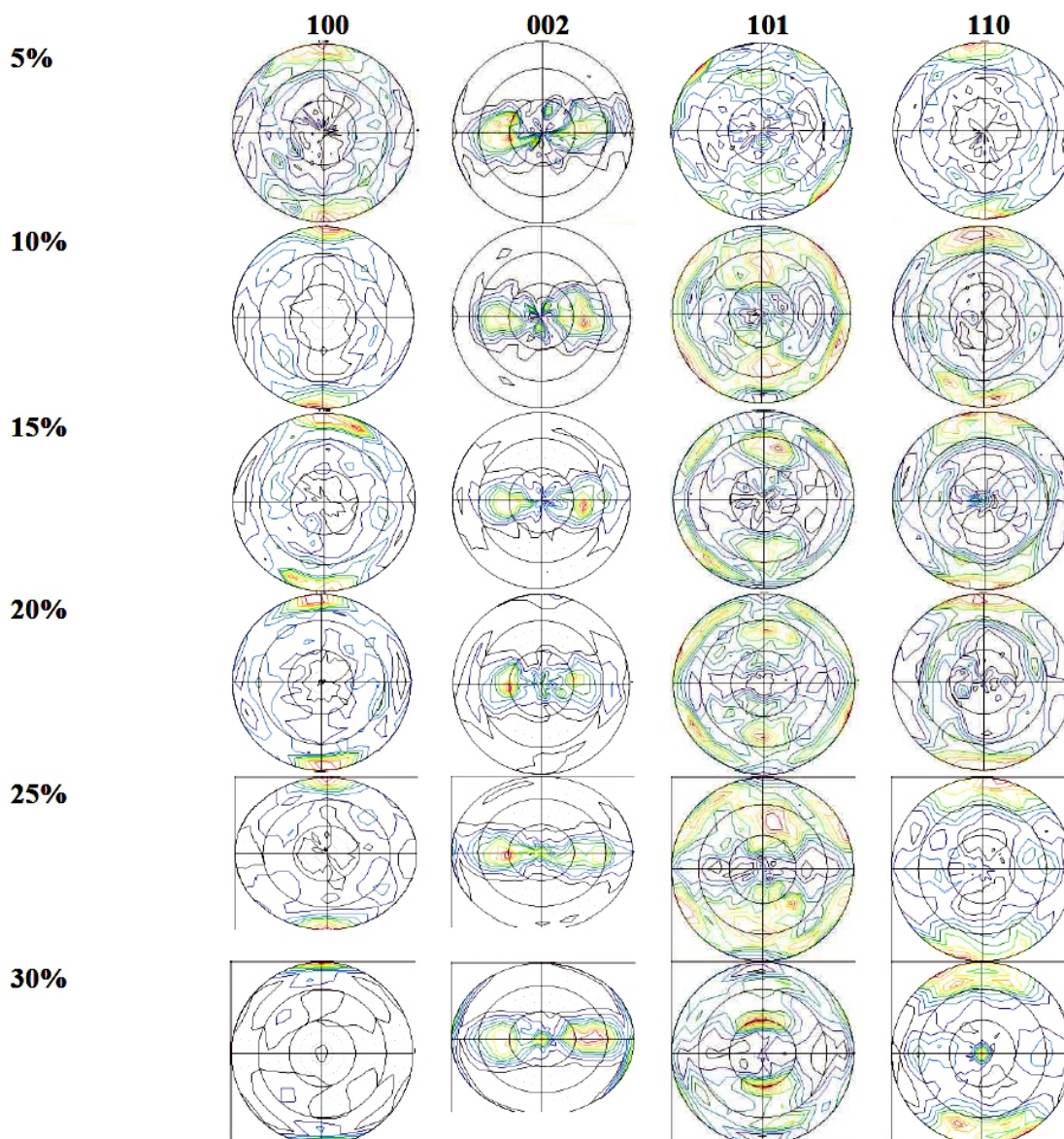
Roviny (101) byly původně ( $e = 5\%$ ) orientovány kolmo k transversálnímu směru (obrázek 2), během deformace tahem však dochází k jejich stáčení o 45° od TD směrem k RD (tabulka 1).



Obrázek 2. Vypočtené inverzní pólové obrazce.



Tabulka 1. Přímé pólové obrazce.



## Literatura

- Murty, K. L.: Applications of Crystallographic Textures of Zirconium Alloys in the Nuclear industry, Zirconium in the nuclear industry: Eighth International Symposium, ASTM STP 1023, L.F.P. Van Swam and C.M. Eucken, Eds. , American Society for testing and Materials, Philadelphia, 1989, pp. 570 – 595.
- Dlouhá, M., Kalvoda, L., Vratislav, S., Cech, B.: Texturní analýza trubek ze zirkoniových slitin neutronovou difrakcí, Kovové materiály 4.29, Bratislava, 1991.
- Laboratoř neutronové difrakce KIPL FJFI, Praktikum ze struktury pevných látek: Třídímní texturní analýza kubických materiálů pomocí ODF (programový soubor CUBIC), Faculty of Nuclear Science and Physical Engineering, Praha, 1985.
- Tenckhoff, E.: Review of Deformation Mechanism, Journal of ASTM International JAI, 2(2005).
- Krůželová, M.: Studium vlastností slitin na bázi zirkonia metodou neutronové difrakce, České vysoké učení technické v Praze, 2012 (diplomová práce).
- G.B. Harris. Philos Mag, 43, 1952, p. 113.
- A.C. Larson, R.B. Von Dreele, General Structure Analysis System (GSAS), Los Alamos National Laboratory Report LAUR 86-748, 1994.

SL11

## TWINNING EVOLUTION AS A FUNCTION OF LOADING DIRECTION IN MAGNESIUM

J. Čapek, K. Máthis

Department of Physics of Materials, Faculty of Mathematics and Physics, Charles University, Ke Karlovu 5, 121 16 Prague, Czech Republic

**Keywords:** magnesium, twinning, neutron diffraction

### Introduction

Unique properties of magnesium alloys predestine them for many applications. Especially transportation industry takes advantage of their low density and high specific strength. Owing to their hexagonal close packed (HCP) structure and  $c/a$  ratio close to ideal value the deformation behavior differ from the other, e.g. fcc or bcc metals. The lowest value of critical resolved shear stress (CRSS) is for basal slip  $(0001) \frac{1}{2} \bar{1}1\bar{2}0$ , followed by prismatic slip  $(10\bar{1}0) \frac{1}{2} \bar{1}1\bar{2}0$  and the first  $(10\bar{1}1) \frac{1}{2} \bar{1}1\bar{2}0$  and second-order  $(1\bar{1}\bar{2}2) \frac{1}{2} \bar{1}1\bar{2}3$  pyramidal slip system [1]. Combination of all systems having (i.e.  $\frac{1}{2} \bar{1}1\bar{2}0$ ) provides only 4 independent slip systems. Therefore, the von Mises criterion requiring five independent slip systems for homogenous deformation is not fulfilled and activation of second-order pyramidal system or mechanical twinning is necessary. Since activation of second-order pyramidal system requires high stresses or high temperatures, mechanical twinning is the preferred deformation mechanism at room temperature.

In magnesium, the most easily activated twinning mode is  $(10\bar{1}2) \parallel 10\bar{1}1$  extension twinning. The twinning on  $\{10\bar{1}2\}$  plane causes reorientation of the lattice by  $86.3^\circ$  and extension along the  $c$ -axis of the twinned grain. Owing to its polar nature different grains undergo twinning during tensile and compressive deformation and different deformation texture evolution is observed.

In the present paper the twinning evolution is studied using in-situ neutron diffraction technique. The main advantage of this method is in its capability to examine large sample volume owing to the deep penetration length of thermal neutrons. Furthermore, the intensity changes of

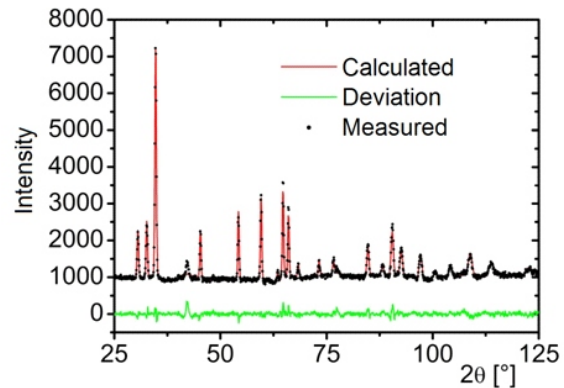


**Figure 1.** Measured ND pattern of initial state compared with ideally random distribution.

particular diffraction peaks characterize the twinning and shift of diffraction peaks provides information about lattice deformation and internal stresses. The overall twinned volume can be determined from the intensity variations of particular peaks, caused by the crystal lattice reorientation during the twinning [2-5].

### Experimental technique

Cast polycrystalline magnesium with 1 wt.% Zr content was used for the experiment. Zirconium additive stabilize the grain size to the value of  $110 \text{ nm}$ . The ND measurement showed that the initial samples have random grain orientation distribution. (Fig. 1) The monotonic compression and tensile tests was applied at room temperature at a strain rate of  $\dot{\epsilon}$ . The test was stopped for approx. 70 min at particular strain values in order to collect the neutron diffraction data.

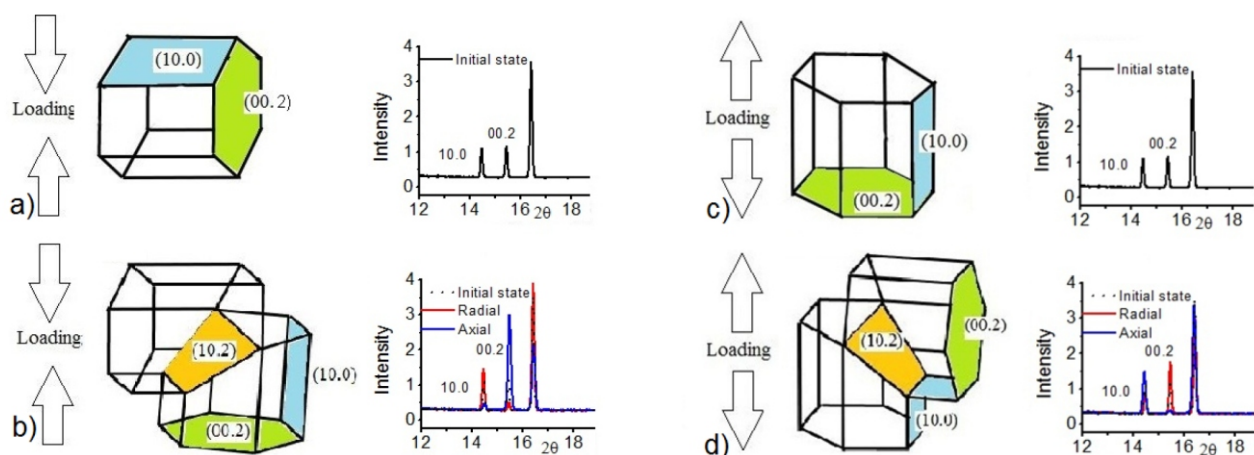


**Figure 2.** Comparison of ND pattern of initial state (a,c) and after compression (b) and tension (d).

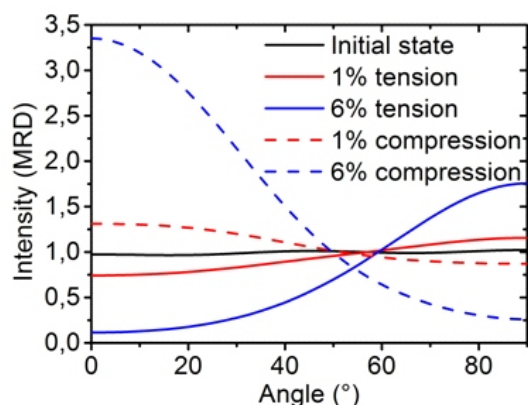


**Figure 3.** Distribution of 0002 plane before and during deformation.

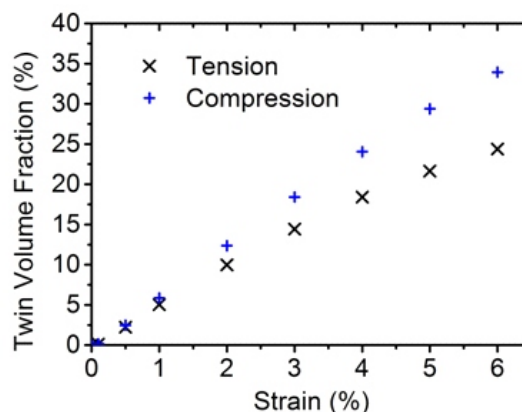


**Figure 4.** Twin volume fraction as a function of strain.

The SMARTS engineering instrument at LANSCE [6] was used for collecting the diffraction pattern. The diffraction patterns were measured using two detector banks at  $\pm 90^\circ$  to incident beam. The angle between the incident beam and the loading direction was  $45^\circ$  [7]. This setup provides diffraction measurement of crystallographic planes both perpendicular and parallel to the loading direction.

The  $\{00.2\}$ – $\{10.0\}$  parent-daughter system characterize well the twinning activity [8] owing to the following reason: in tension those grains are ideally oriented for twinning, which normal of the basal plane is parallel with the loading direction. In the initial state those grains contribute to the 0002 peak. As extension twinning occurs, part of the grains reorients by almost  $90^\circ$  and consequently increase of the  $10\bar{1}0$  peak can be observed. Since in compression the grains having their  $c$ -axis perpendicular to the loading axis are optimally oriented for extension twinning, the intensity changes have opposite sense (Fig. 2).

## Results

As demonstrated in [7], the determination of the twin volume fraction during the deformation is possible from the diffraction data by performing a 2-bank Rietveld refinement assuming an axisymmetric texture. The initial texture is random in the present case, and the uniaxial deformation is an axisymmetric operation, and hence the assumption should be valid. The refinements were done using the GSAS [9] and SMARTSware [10] software packages developed at Los Alamos National Laboratory. The axial distribution function was calculated for the 00.2 peak during deformation. The 0002 distribution is almost random at the start. When external stress is applied, the distribution of 0002 plane starts to change due to the twinning (Fig. 3). From the changes in the area under the curve above (tension) and below (compression) the cross-over point we can directly determine the twin volume fraction as described in [7]. Fig. 4 shows the twin volume fraction as a function of the absolute value of the applied strain for the tension and compression samples. In the entire range the twin volume fraction is larger for compression than it is for tension.

## References

1. J.W. Christian, S. Mahajan, *Prog Mater Sci* 39 (1995) 1-157.
2. M.A. Gharghouri, G.C. Weatherly, J.D. Embury, J. Root, *Philos Mag A* 79 (1999) 1671-1695.
3. S.R. Agnew, D.W. Brown, C.N. Tome, *Acta Mater* 54 (2006) 4841-4852.
4. O. Muránsky, M.R. Barnett, D.G. Carr, S.C. Vogel, E.C. Oliver, *Acta Mater* 58 (2010) 1503-1517.
5. O. Muránsky, D.G. Carr, P. Šittner, E.C. Oliver, *Int. J Plasticity* 25 (2009) 1107-1127.
6. M.A.M. Bourke, D.C. Dunand, E. Ustundag, *Appl Phys A-Mater* 74 (2002) S1707-S1709.
7. B. Clausen, C.N. Tome, D.W. Brown, S.R. Agnew, *Acta Mater* 56 (2008) 2456-2468.
8. D.W. Brown, S.R. Agnew, M.A.M. Bourke, T.M. Holden, S.C. Vogel, C.N. Tome, *Mat Sci Eng A-Struct* 399 (2005) 1-12.
- [9] R.B. Von Dreele, J.D. Jorgensen, C.G. Windsor, *J Appl Crystallogr* 15 (1982) 581-589.
- [10] B. Clausen, SMARTSware manual, The Regents of the University of California, Los Alamos, 2003.

## Acknowledgements

*The authors are grateful for the financial support of the Czech Science Foundation under the contract P204/12/1360. JČ acknowledges the support from the Grant Agency of Charles University under contract Nr. 513512.*

SL12

**STUDY OF MAGNESIUM COMPOSITES BY NEUTRON DIFFRACTION METHOD****G. Farkas<sup>1</sup>, K. Máthis<sup>1</sup>, Z. Száraz<sup>2</sup>**<sup>1</sup>*Department of Physics of Materials, Charles University, Ke Karlovu 5, 121 16 Prague, Czech Republic*<sup>2</sup>*The University of Manchester, Oxford Road, Manchester M13 9PL UK  
farkasgr@gmail.com*

Neutron diffraction has been applied to investigate lattice deformation and internal stresses in magnesium alloy Mg-5wt.%Al -1wt. %Sr (AJ51) reinforced with short Saffil® fibers Al<sub>2</sub>O<sub>3</sub> with volume fraction 18% deformed in compression at room temperature. Lattice strain was calculated from position changes of diffraction peak {10.1} by using the Bragg equation.

The residual stress was measured with ex-situ neutron diffraction in the axial and radial direction with respect to the loading axis. It was found that in the matrix phase at initial state tensile residual stress is present in the matrix. In axial direction tensile residual stress evolution in matrix phase shows inverse behavior; it increases with applied compressive deformation. In radial direction the residual stress exhibits significant changes only at the beginning of deformation, during further deformation stays constant within the experimental error.

In-situ neutron diffraction was used for determining lattice strain in axial detector direction in samples with two different fiber orientations. The measurements revealed more intensive plastic deformation in the matrix for perpendicular fiber orientation, which is in agreement with the shear lag model [1], describing the load transfer from the matrix to the fibers.

*The authors are grateful for the financial support of the Czech Science Foundation under the contract P108/12/J018. GF acknowledges the support from the Grant Agency of Charles University under contract Nr. 676112.*

1. R. M. Aikin, L. Christodoulou, Scripta Metall. Mater., 25, 1991, p. 9.

SL13

**SHAPE MEMORY ALLOYS PREPARED BY VARIOUS METHODS****J. Kopeček<sup>1</sup>, M. Jarošová<sup>2</sup>, K. Jurek<sup>2</sup>, L. Bodnárová<sup>3</sup>, H. Seiner<sup>3</sup>, P. Sedlák<sup>3</sup>,  
M. Landa<sup>3</sup>, J. Drahokoupil<sup>1</sup>, F. Laufek<sup>4</sup>, P. Novák<sup>5</sup>, M. Dopita<sup>6</sup>, V. Kopecký<sup>1</sup>,  
O. Heczko<sup>1</sup>**<sup>1</sup>*Institute of Physics of the AS CR, Na Slovance 2, 182 21 Praha 8, Czech Republic*<sup>2</sup>*Institute of Physics of the AS CR, Cukrovarnická 10/112, 162 00 Praha 6, Czech Republic*<sup>3</sup>*Institute of Thermomechanics of AS CR, Dolejškova 5, 182 00 Prague 8, Czech Republic*<sup>4</sup>*Czech Geological Survey, Geologická 6, 152 00 Praha 5, Czech Republic*<sup>5</sup>*Institute of Chemical Technology, Dept Met & Corros Engrn, Technická 5, 16628 Praha, Czech Republic*<sup>6</sup>*Technical University Bergakademie Freiberg, Inst. Mat. Sci., D-09596 Freiberg, Germany*

Shape memory alloys have been investigated for couple of last decades in IoP ASCR. Main attention has paid to investigation of the single-crystals to describe martensitic transformation properly after some years of polycrystals properties studies. Nevertheless, progress of knowledge turn attention toward applied problems as well and thus polycrystalline became investigated again. Novel procedures of powder metallurgy as spark plasma sintering (SPS), self-combustion high-temperature synthesis (SHS) and mechanical alloying are applied now.

I would like to present the compilation of recent results, which were performed on two materials. The first one is less common SMA Co<sub>38</sub>Ni<sub>33</sub>Al<sub>29</sub>, which was studied as single crystals and SPS prepared samples. The martensitic

transformation in this alloy was quite underestimated by other authors in last decades and some details of transformation kinetics are not documented even now.

The second one is the cornerstone of SMAs – the NiTi alloy here prepared by combination of SPS and SHS processes, when the ignition of SHS is done in SPS machine chamber. Such process should help the convenient preparation of Nitinol thin wires for medical applications. It can avoid the creation of particles, especially carbides, which precipitates during all casting processes as are VIM and VAR.

*Authors would like to acknowledge the financial support from the Czech Science Foundation projects 101/09/0702 and 14-03044S.*